IOP Conference Series: Earth and Environmental Science

Investigations of turbulent flows in a tubular pump and structural stresses of its impeller

To cite this article: X L Tang *et al* 2012 *IOP Conf. Ser.: Earth Environ. Sci.* **15** 052012

IOP Conf. Series: Earth and Environmental Science **15** (2012) 052012 doi:10.1088/1755-1315/15/5/052012

Investigations of turbulent flows in a tubular pump and structural stresses of its impeller

X LTang[1], Y X Jia[1], F J Wang[1], D Q Zhou[2], R F Xiao[1] W Yang[1] and Y L Wu[3]

[1] College of Water Resources & Civil Engineering, China Agricultural University, 17 Qinghua Donglu Haidian District, Beijing, 100083, China
[2] College of Energy and Electrical Engineering, Hohai University, 1 Xikang Road, Nanjing, 210098, China
[3] State Key Laboratory of Hydroscience and Engineering, Tsinghua University, Haidian District, Beijing, 100084, China

E-mail: xl-tang@mail.tsinghua.edu.cn

Abstract. Based on Navier-Stokes equations and RNG k-ε turbulence model, numerical simulation was carried out to investigate turbulent flows in tubular pumps and structural stresses of its impeller using commercial software of ANSYS Workbench. Firstly, the calculated velocity and pressure distributions in tubular pumps show that the whole flow pattern is uniform except for that in the region in the front of the pier in the discharge passage. The predicted spiral streamlines in the front of the discharge passage indicate that there exists an unrecovered velocity circulation. The computed reasonable distributions of the static pressure show the minimum happens at inlet edges on the suction surfaces of the blades which probably causes cavitations. One-way fluid-structure interaction method was then employed to make a further static structural analysis of the impeller, and the predicted stresses and deformations of the blades show that the maximal equivalent stress exists in the joint between the blades and the hub on pressure surfaces of the impeller, the maximum of total deformations of the blades increases as the radius increases. The maximal exists near the impeller rim at the inlet and outlet edges. The calculated results will provide references for further design and research of tubular pumps.

1. Introduction

The South-to-North Water Transfer Project is a strategic infrastructure project related to sustainable development of economy and environment in the Plain of the Yellow River, Huai and Hai Rivers in China. Tubular pumps are applied widely in low-head pump stations due to their characteristics of the simple structure, less investment, uniform flow pattern, which are becoming the focuses for scholars. Zhu et al. [1] studied the flow fields in a front-positioned shaft tubular pump and a rear-positioned one respectively, and the calculated results show that the size and shape of the shaft affect the head losses inside the discharge passage and the efficiency of pumping system when the shaft is rear-positioned. After turning the impeller 180 degrees along its axis and keeping the original passages, the hydraulic losses inside both suction passages and discharge passages increase, and the range of high efficiency moves toward smaller flow rates. By simulating the initial scheme of the large shaft tubular-pump station in Guangdong Province, Xiao et al. [2] put forward a optimal scheme of passages size to obtain a reasonable flow pattern inside the overall passages, which reduces the shock of strong flow against the pump inlet and eliminates the reverse flows, the negative pressures as well as the flow separations.

Jin et al. [3] focused on the static pressure distributions on blade surfaces and the relative velocity distributions near the cross-sections of the airfoil under different operating conditions and found that the major proportion of hydraulic losses happens inside the guide vane and the bulb unit, and the simulated results agree closely with experimental data nearby the range of high efficiency while they deviate from the experimental at low or high flow rates. Liu et al. [4] simulated various operating cases under conditions of 16 different discharges ranging from 50% to 120% of the design flow rate in front-positioned and rear-positioned shaft tubular-pump, and analyzed the flow pattern in the suction and discharge passages. The predicted flow pattern of front-positioned shaft tubular-pump is uniform in suction and discharge passages while that of the rear-positioned is disorder in discharge passages with higher hydraulic losses.

Impellers are the key components of the tubular pump and their strength properties are very important for the operating safety of the whole unit. Zheng et al. [5] carried out numerical simulation of the three dimensional flow around an axial-flow runner using the finite volume method and unstructured grid systems, and then performed the rigidity/strength analysis of the runner blades by applying the water pressure load on the blade surfaces. According to computational results among the whole range of flow rates, the stresses and distortion reach the maximal at the operating point of the rated output power for the maximal head. Chen et al. [6] analyzed the blade stresses in reactor coolant pump of a 300MW nuclear power plant in China and found that the maximal equivalent stress exists in fixed supports and the blade stress distributions are not strictly periodic. In order to calculate accurately the stresses and deformations of the stamping and welding impeller in the flow field, Wang et al. [7] analyzed the fluid-structure interaction inside a centrifugal pump impeller by adopting one-way method. The calculated results show that the stress of the impeller is markedly uneven and the stress concentration appears locally. The total deformations of the impeller increases as the radius increases and it reaches the maximum at the rim of the blades.

Based on the FLUENT software, numerical simulation was carried out in the overall passage in the front-positioned shaft tubular pump, and the pressure distributions on the blade surfaces and the overall streamlines are obtained. One-way fluid-structure interaction is then adopted to analyze the dynamic characteristics of the impeller, and the static stress distributions and the total deformation distributions of blades under different flow rates are achieved. All of the results provide references for the safe operation of tubular pumps.

2. Numerical methods

2.1. Calculation methods of flow field

The internal flows in pumps are complex 3D unsteady and incompressible turbulent flows which can be described using continuity equation and momentum equations expressed in a fixed coordination as follows:

$$\frac{\partial \rho}{\partial t} + \nabla \cdot (\rho \boldsymbol{u}) = 0 \tag{1}$$

$$\frac{\partial \rho \boldsymbol{u}}{\partial t} + \nabla \cdot (\rho \boldsymbol{u}\boldsymbol{u} - \tau) = \boldsymbol{F}^{\boldsymbol{B}} \tag{2}$$

where, ρ represents fluid density; $\boldsymbol{u}$ is the velocity vector; τ is the stress tensor; $\boldsymbol{F}^{\boldsymbol{B}}$ represents the body force vector of fluid. Furthermore, the N-S equations in a rotating coordinate can be rewritten as:

$$\frac{\partial \rho}{\partial t} + \nabla \cdot (\rho \boldsymbol{u}_r) = 0 \tag{3}$$

$$\frac{\partial \rho \boldsymbol{u}_r}{\partial t} + \nabla \cdot (\rho \boldsymbol{u}_r \boldsymbol{u}_r - \tau) = \boldsymbol{F}^{\boldsymbol{B}} + \boldsymbol{F}_c \tag{4}$$

In which, $\boldsymbol{u}_r$ is the relative velocity and $\boldsymbol{F}_c$ is the additional force [8].

2.2. Structural stress calculation methods

The static structural stress analysis is used to calculate the displacement, stresses, strains and forces caused by the constant forces loaded on structures or components of the pump under conditions of steady operating cases.

The following is the structural dynamic equilibrium equation based on linear finite element method:

$$\left[M\right]\{\ddot{u}\}+[C]\{\dot{u}\}+[K]\{u\}=\{F\} \tag{5}$$

where $\left[M\right]$, $[C]$, $[K]$ are mass matrix, damping matrix and stiffness matrix, respectively; $\{\ddot{u}\}$, $\{\dot{u}\}$ and $\{u\}$ are the acceleration, the velocity, and the displacement of the node in finite elements, respectively; $\{F\}$ stands for the load vector, including the pressure, the gravity and centrifugal force of the node[9].

After the structure equations are discretized, the overall stiffness equations are solved to obtain the each unit stress $\{\sigma\}$ according to the principle of virtual work:

$$\delta U=\delta V \tag{6}$$

$$\{\sigma\}=K[W_n] \tag{7}$$

where, U represents virtual deformation energy; V represents the virtual work done by external force $\{F\}$; K represents the stiffness matrix of each element; $[W_n]$ represents the normal displacement.

2.3. Solution processes of fluid-structure interaction

Fluid-structure interaction is a process of iterating equations. Firstly the initial coupling boundaries are assumed, and then the flow equations are solved to obtain the pressure distributions on the surfaces of the fluid region on coupling boundaries, and thus the pressure is regarded as the forces imposed on the structure of the pump, which is regarded as the force boundaries for solution iteration of structural dynamic equations. Finally the stresses and deformations are obtained. Recent years, researchers have applied this method in the fluid machinery successfully [10-13]. This study only takes into account the structure deformations under the influence of the fluid ignoring the reaction of the structure to the fluid because of the small deformations for the low-head tubular pumps.

3. Physical model and boundary conditions

Shaft front-positioned tubular pumps consist of the inlet passage, the impeller, and the diffuser and the discharge passage. The impeller diameter is 300 mm with 3 blades and blade angle of 0°, and the diffuser has 6 blades. The design flow rate for pump model is 0.28099 m^3/s, and the rotational speed is 1078 r/min. The whole model scale is 1:11. The computational zones of pump model are shown in figure 1. The total number of computational elements of the whole passage is 1,850,000, and the number of computational elements of impeller structural model is 330,000. The 3D modeling of the pump is shown in figure 2, and the unstructured grids of the impeller passage and the diffuser passage are shown in figure 3.

Numerical simulation of the whole passage was conducted based on FLUENT software to provide a more accurate pressure load for the static structural analysis. A constant axial velocity based on the mass flow rate is specified at the inlet of the passage, and the gradients of the pressure at the outlet are set to zero. All physical surfaces are set to no-slip wall and interfaces are set to connect the computational zones. The material of the impeller is structural steel with density of 7850 kg/m^3; the modulus of elasticity is 2×10^5 MPa; the Poisson's ratio is 0.3 and ultimate tensile strength is 4.6×10^8 Pa. The fluid is water with density of 1000 kg/m^3 and the gravity acceleration is 9.8 m/s^2. The RNG k-ε turbulence model is adopted to close the time-averaged incompressible Navier-Stokes equations to simulate the internal flows. Compared with the standard turbulence model, this model considers the rotating and swirling flow, which can better handle the flow with a high strain rate and streamlines of high curvature. The SIMPLEC algorithm is used for pressure and velocity equations coupled. Second-order upwind format is set for turbulent kinetic energy and dissipation rate, and standard difference is set for pressure strength.

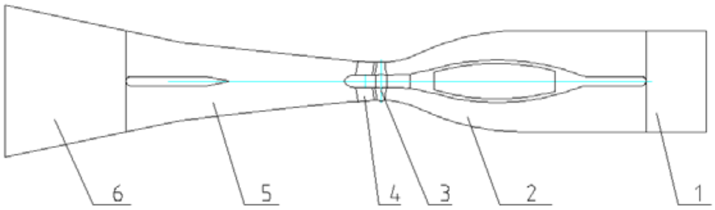

Figure 1. Computational domain of the pump model: 1. Extension to suction passage 2. Suction passage 3. Impeller passage 4. Diffuser passage 5.Discharge passage 6. Extension to discharge passage

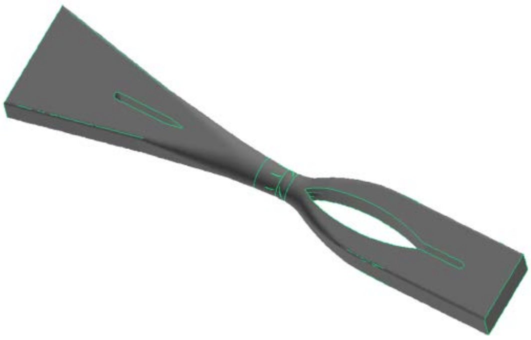

Figure 2. 3D modeling of the pump

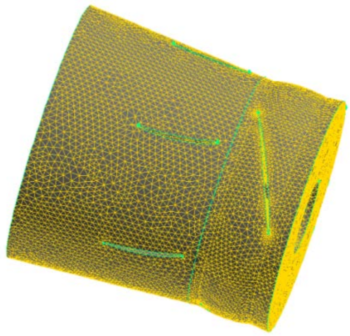

Figure 3. Grids of impeller and diffuser passage domain

4. Result analyses

In order to analyze comprehensively the stresses and deformations of the tubular pump impeller, the numerical simulation was performed to calculate the overall flow field under conditions of nine operating cases, and then the pressure load on the surfaces of the blades was exerted on the impeller structure to make further finite element analysis using ANSYS Workbench software.

4.1. Analyses of flow field

4.1.1. *External characteristics comparison.* Different operating conditions were simulated using FLUENT to obtain the external characteristics, and the following equations are used to calculate the head and efficiency of the pump.

$$H = (p_{out} - p_{in}) / \rho g \tag{8}$$

$$\eta_h = \rho g Q H / M\omega \tag{9}$$

$$\eta = \eta_h \eta_m \eta_v \tag{10}$$

In which p_{in} and p_{out} represent the total pressure of inlet and outlet respectively. ρ is the density of water, g is gravity acceleration, H is the calculated head, Q is volumetric flow rate, M is the torque of impeller, ω is angular velocity, η_m is the mechanical efficiency equal to 0.97 and η_v is the volumetric efficiency equal to 0.98.

The calculated performance curves were illustrated to make a contrast with experimental data in Fig. 4. It can be seen that the calculated values agree well with experimental data in the overall trend, the simulated heads are slightly higher than the experimental, but the relative error remains within 5% probably due to the numerical simulation not considering the clearance between the blades and the hub as well as that between blades and the passage, which leads to the calculated hydraulic losses lower than the real values. As a result, the heads and shaft powers are higher than the experimental and the efficiencies are lower than the experimental data, but the efficiency error remains within 10%.

4.1.2. *Flow pattern and pressure distributions of blades.* Figure 5 and Figure 6 show the streamlines and the pressure distributions on the axial cross-section of the whole passage at the design flow rate respectively. The calculated velocity and pressure distributions in the tubular pump show that the whole flow pattern is uniform except for that in the region in the front of the pier in the discharge passage. The corresponding spiral streamlines in the front of discharge passage was predicted, indicating that there exists an unrecovered velocity circulation. As can be seen from Fig. 7, the computed reasonable distributions of the static pressure illustrate that the minimum happens at inlet edges on the suction surfaces of the blades, which probably causes cavitations.

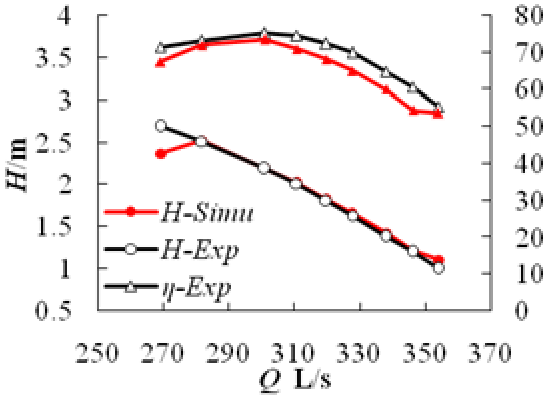

(a) Head and efficiency vs discharging curves

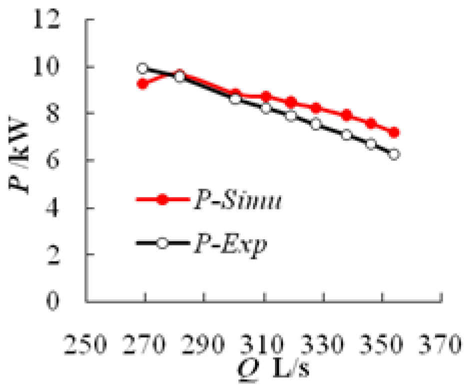

(b) Shaft power vs discharging curves

Figure 4. Comparison of computational external characteristics with experimental data

In a word, the above-mentioned numerical techniques can be used to predict accurately the characteristics of the tubular pump and the pressure distributions on the impeller surfaces, which provides a guarantee for the static structural analysis.

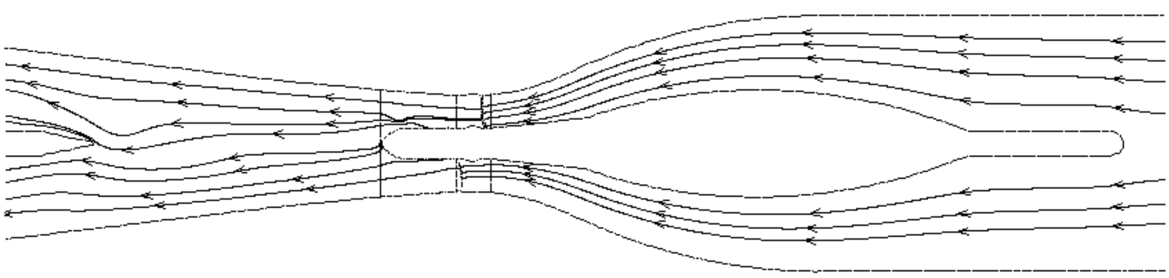

Figure 5. Streamlines distribution on the axial cross-section of the whole passages

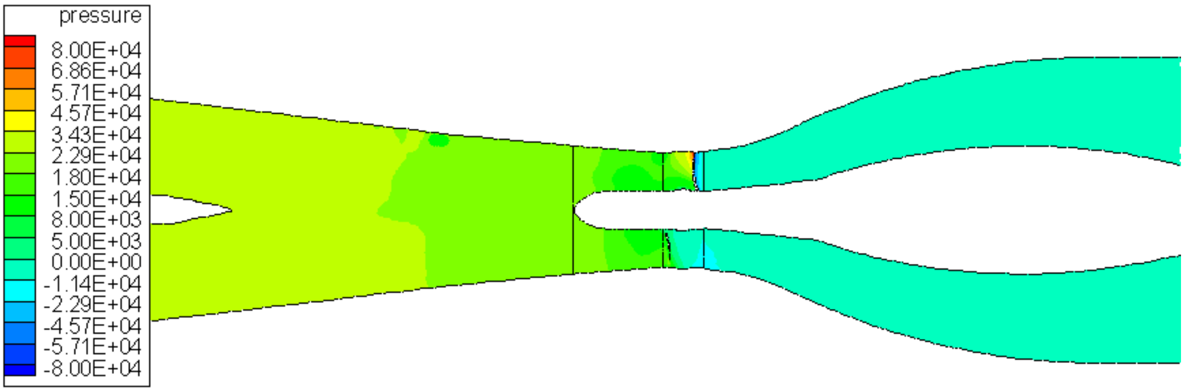

Figure 6. Pressure distributions on the axial cross-section of the whole passage

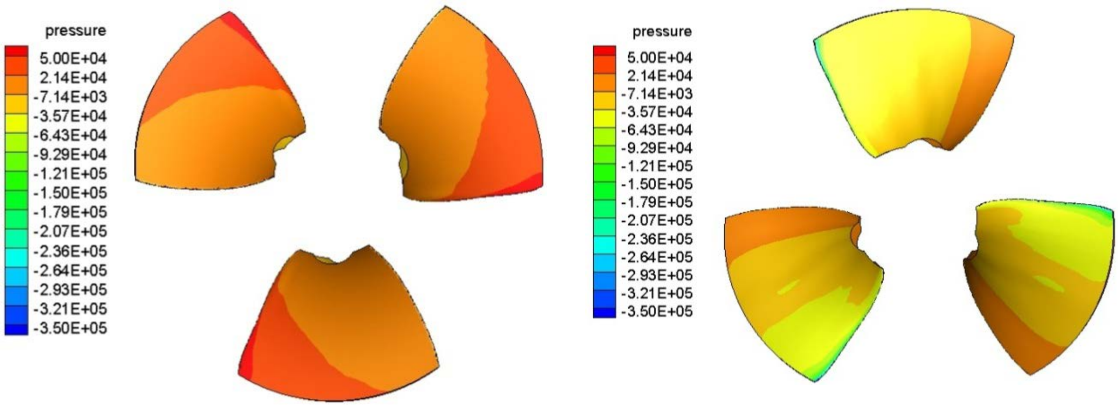

(a)Pressure distributions on the pressure surfaces

(b) Pressure distributions on the suction surfaces

Figure 7. Pressure distributions on the blade surfaces

4.2. Analyses of static stress

By performing the finite element solution of the impeller, the maximal equivalent stresses and the maximal total deformations are obtained under different conditions shown in figure 8. It can be found that total deformation amount reduces with the flow rate increasing and the equivalent stress fluctuates in irregularity. Both the maximums of equivalent stress and the max total deformation appear at the design flow rate. As shown in figure 4, both the shaft power and the head reach the maximum at the design condition, which explains the reason for both the maximums of the equivalent stress and the total deformations shown in figure 8. The maximum of equivalent stress is 265.3MPa and the ultimate tensile strength is 460MPa, so this impeller meets the strength requirements.

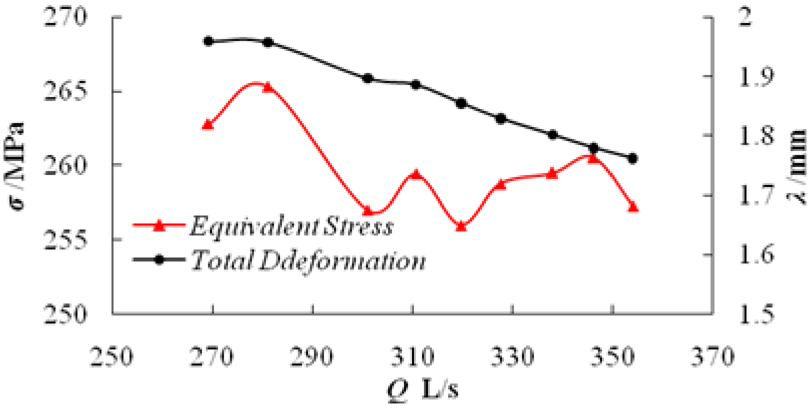

Figure 8. Total deformations and equivalent stress under different operating conditions

Because the equivalent stresses and total deformation distributions are similar under different operating conditions, the equivalent stress and total deformation distributions only under design flow rate are shown in figure 9 and figure 10 respectively. It can be seen that the force on the impeller is uneven, the equivalent stresses reduce with the radius increasing, and the equivalent stresses on pressure surfaces are slightly higher than that on the suction surfaces. The concentrated stress appears at the joint between the blades and the hub. The actual cause can be interpreted as follows: the tubular pump impeller is designed using the design method for axial-flow pump impellers, and the impeller blades are the cantilever structure and the flow impact happens on the blade surfaces, which causes the pressure surfaces to be under tension and the suction surfaces to be under pressure. So the concentrated tension stress is greater than the compressive stress, and the pressure at the outlet edges is greater than that at the inlet edges. It is found from figure 10 that the total deformations are not uniform either and increase as the radius increases, and its maximum is 1.9574mm, which exists at the rim of impeller nearby inlet inlet. The cause is that the centrifugal force is highest at the rim of the blades and the flow impact also exists at the inlet edges due to the blade angle of attack.

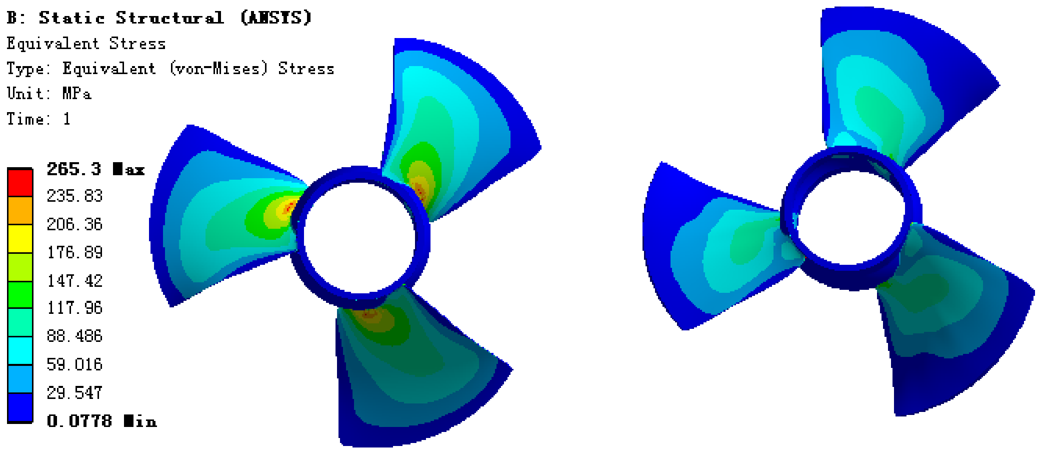

(a) The pressure surfaces (b) The suction surfaces

Figure 9. Equivalent stress distributions on the impeller

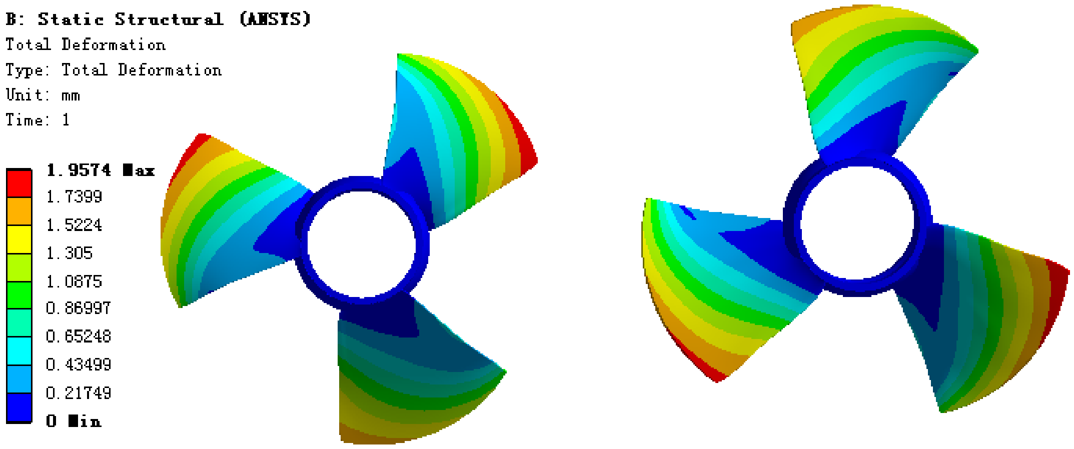

(a) The pressure surfaces (b) The suction surfaces

Figure 10. Total deformation distributions on the impeller

5. Conclusions

The numerical simulation of flow field and the static structural stress analyses for the front-positioned shaft tubular pump were conducted to obtain the external characteristics of the pump and the structural dynamic characteristics, respectively. It proves that the pump design method is validated by comparing the calculated results with the experimental data. Based on the ANSYS Workbench software, the finite element solution was performed by exerting pressure load on the impeller structure to obtain the equivalent stresses and total deformations. The conclusions can be drawn as follows:

(1) The computational results have the same overall trend as the experimental, the computed heads and the computed shaft powers are higher than the experimental, and the predicted efficiencies are lower than the experimental under different operating conditions. The reason for the difference between the computed and the experimental is that the numerical simulation does not consider the tip clearance between blades and the hub as well as that between blades and the impeller passage.

(2) The equivalent stresses and the total deformations reach the maximums at the design flow rate corresponding to the maximum head and the maximum shaft power. The maximum of equivalent stress is 265.3MPa, which is lower than the ultimate tensile strength 460MPa of structural steel, so the impeller design meets the material requirements. The equivalent stress reduces as the radius increases and the concentrated stress appears at the joint between the pressure surfaces and the hub. The total deformations increase as the radius increases and the maximum of the total deformation appears at the rim of the blades nearby the inlet and the outlet regions.

Acknowledgments

This Project is supported by the Program for New Century Excellent Talents in University (NCET) (Grant No. NETC-10-0784) and the National Natural Science Foundation of China (50976124, 51179192 and 51139007).

References

[1] Zhu H G, Zhang R T, Yao L B and Wei J 2011 Numerical analysis of shaft tubular pumping systems *Int. Conf. on Computer Distributed Control and Intelligent Environmental Monitoring(Changsha, China, Feburary 19-20, 2011) 491-495*
[2] Xiao Y P, Zheng Y, Jiang R H, Liu M Q and Liu J 2010 *Water Resources and Power* **28** 143-145
[3] Jin Y, Liu C and Tang F P 2010 *J. of Mechanical Engineering* **46** 167-174

[4] Liu J, Zheng Y, Zhou D Q, Mao Y T and Zhang L M 2010 *Transactions of the Chinese Society for Agricultural Machinery* **41** 32-38
[5] Zheng X B, Luo X Q and Wu H J 2006 *J. of Hydroeletric Engineering* **25** 121-124
[6] Chen X Y, Yuan D Q, Yang M G and Yuan S Q 2010 *J. of Mechanical Engineering* **46** 111-114
[7] Wang Y, W H Y, Zhang X and Xu X M 2011 *Transactions of the Chinese Society for Agricultural Machinery* **27** 131-136
[8] Wang X and Luo S Z 2010 Vibration analysis of large bulb tubular pumping station considering flow-structure interaction APPEC 2010 (Chengdu, China, March 28-31, 2010) 1-4
[9] Zhao W 2008 Study on Fluid-structure Interaction for Large Hydraulic Turbines *Master Thesis* (Beijing: China Agricultural University)
[10] Wang W Q, He X Q, Zhang L X, Liew K M and Guo Y 2009 *Int. J. for Numerical Methods in Fluids* **60** 515-538
[11] Münch C, Ausoni P, Braun O, Farhat M and Avellan F 2010 *J. of Fluids and Structures* **26** 1018-33
[12] Ahmadi A and Keramat A 2010 *J. of Fluids and Structures* **26** 1123–41
[13] Campbell R L 2010 Fluid–structure Interaction and Inverse Design Simulations for Flexible Turbomachinery *PhD. Thesis* (Pennsylvania State: The Pennsylvania State University)